This is the accepted manuscript version of the contribution published as:

Heinze, B.M., Küsel, K., **Jehmlich, N.**, **von Bergen, M.**, Taubert, M. (2023):
Metabolic versatility enables sulfur-oxidizers to dominate primary production in groundwater
Water Res. **244** , art. 120426

The publisher's version is available at:

https://doi.org/10.1016/j.watres.2023.120426

Water Research xxx (xxxx) 120426

Contents lists available at ScienceDirect

Water Research

journal homepage: www.elsevier.com/locate/watres

Metabolic versatility enables sulfur-oxidizers to dominate primary production in groundwater

Beatrix M. Heinze [a], Kirsten Küsel [a, b, c], Nico Jehmlich [d], Martin von Bergen [b, d, e], Martin Taubert [a, c, *]

[a] Aquatic Geomicrobiology, Institute of Biodiversity, Friedrich Schiller University Jena, Dornburger Str. 159, Jena 07743, Germany
[b] The German Centre for Integrative Biodiversity Research (iDiv) Halle-Jena-Leipzig, Puschstr. 4, Leipzig 04103, Germany
[c] Cluster of Excellence Balance of the Microverse, Friedrich Schiller University Jena, Jena, Germany
[d] Department of Molecular Systems Biology, Helmholtz Centre for Environmental Research, UFZ, Permoserstr. 15, Leipzig 04318, Germany
[e] Faculty of Biosciences, Pharmacy and Psychology, Institute of Biochemistry, University of Leipzig, Brüderstr. 32, Leipzig 04103, Germany

ARTICLE INFO

Keywords:
Chemolithoautotrophy
Groundwater
Sulfur-oxidizing bacteria
^{13}C-CO_2 stable isotope probing
Genome-resolved metaproteomics
Metagenomics

ABSTRACT

High rates of CO_2 fixation and the genetic potential of various groundwater microbes for autotrophic activity have shown that primary production is an important source of organic C in groundwater ecosystems. However, the contribution of specific chemolithoautotrophic groups such as S-oxidizing bacteria (SOB) to groundwater primary production and their adaptation strategies remain largely unknown. Here, we stimulated anoxic groundwater microcosms with reduced S and sampled the microbial community after 1, 3 and 6 weeks. Genome-resolved metaproteomics was combined with 50at-% $^{13}CO_2$ stable isotope probing to follow the C flux through the microbial food web and infer traits expressed by active SOB in the groundwater microcosms. Already after 7 days, 90% of the total microbial biomass C in the microcosms was replaced by CO_2-derived C, increasing to 97% at the end of incubation. Stable Isotope Cluster Analysis revealed active autotrophs, characterized by a uniform ^{13}C-incorporation of 45% in their peptides, to dominate the microbial community throughout incubation. Mixo- and heterotrophs, characterized by 10 to 40% ^{13}C-incorporation, utilized the primarily produced organic C. Interestingly, obligate autotrophs affiliated with *Sulfuricella* and *Sulfuritalea* contained traits enabling the storage of elemental S in globules to maintain primary production under energy limitation. Others related to *Sulfurimonas* seemed to rapidly utilize substrates for fast proliferation, and most autotrophs further maximized their energy yield via efficient denitrification and the potential for H_2 oxidation. Mixotrophic SOB, belonging to *Curvibacter* or *Polaromonas*, enhanced metabolic flexibility by using organic compounds to satisfy their C requirements. Time series data spanning eight years further revealed that key taxa of our microcosms composed up to 15% of the microbial groundwater community, demonstrating their *in-situ* importance. This showed that SOB, by using different metabolic strategies, are able to account for high rates of primary production in groundwater, especially at sites limited to geogenic nutrient sources. The widespread presence of SOB with traits such as S storage, H_2 oxidation, and organic C utilization in many aquatic habitats further suggested that metabolic versatility governs S-fueled primary production in the environment.

1. Introduction

Primary production in carbonate aquifers can be as high as in oligotrophic marine systems (Overholt et al., 2022), underlining the substantial contribution of groundwater ecosystems to global C fixation. In the absence of light, CO_2 is exclusively fixed by chemolithotrophic microbes, providing a C source independent from surface inputs or fossil stores. The wealth of metagenomic evidence for chemolithoautotrophy from many groundwater ecosystems supports the high rates of C fixation (Anantharaman et al., 2016; Griebler and Lueders, 2009; Jewell et al., 2016), but the quantitative contribution of specific microbial groups remains unknown.

In groundwater, the world's largest store of liquid freshwater (Gleeson et al., 2016), energy for chemolithoautotrophic CO_2 fixation is provided by inorganic electron donors such as reduced S or N, H_2 or metal ions (Bell et al., 2020; Emerson et al., 2016). Reduced N compounds mostly derive from surface inputs (Albertin et al., 2012), fueling nitrifiers or anaerobic ammonium oxidizers (anammox,(Kumar et al., 2017; Mosley et al., 2022). In contrast, reduced S compounds like thiosulfate or sulfide originate from pyrite minerals in the groundwater

* Corresponding author at: Aquatic Geomicrobiology, Institute of Biodiversity, Friedrich Schiller University Jena, Dornburger Str. 159, Jena 07743, Germany.
E-mail address: martin.taubert@uni-jena.de (M. Taubert).

https://doi.org/10.1016/j.watres.2023.120426
Received 13 May 2023; Received in revised form 25 July 2023; Accepted 27 July 2023
0043-1354/© 20XX

CORRECTED PROOF

Note: Low-resolution images were used to create this PDF. The original images will be used in the final composition.

bedrock (Rimstidt and Vaughan, 2003) or microbial sulfate reduction. With their various redox states, such S compounds can be substrates for both microbial oxidation or reduction (Bell et al., 2020). S-oxidizing bacteria (SOB) generate energy for CO_2 fixation by full or partial S oxidation coupled to aerobic respiration or denitrification (Ghosh and Dam, 2009). This allows SOB to grow chemolithoautotrophically, or as recently shown, mixotrophically in groundwater (Taubert et al., 2022). In fact, the global contribution of SOB to carbon sequestration may be vastly underestimated, as autotrophic SOB can dominate many aquatic habitats, including marine sediments (Boschker et al., 2014; Dyksma et al., 2016), pelagic redox clines (Henkel et al., 2022), and freshwater ecosystems (Hansel et al., 2015; Yang et al., 2011).

Here, we determine the role of SOB for primary production in groundwater of a pristine carbonate aquifer of the Hainich Critical Zone Exploratory (CZE,(Küsel et al., 2016). This site was selected because of its high C fixation rates and putative S-oxidizers constituting around 53% of the chemolithoautotrophic community (Herrmann et al., 2015; Overholt et al., 2022). Rate measurements of N-driven processes like anammox were unable to explain the high C fixation rates, suggesting that SOB are the key primary producers (Overholt et al., 2022). We hypothesize that (I) groundwater SOB are able to dominate primary production in the community and can rapidly respond to reduced S compounds, and following that, (II) hetero- and mixotrophs will assimilate this chemolithoautotrophically produced organic C.

To quantify the assimilation of CO_2-derived carbon into microbial biomass, we employed the recently introduced Stable Isotope Cluster Analysis (SIsCA,(Taubert et al., 2022). This approach allows tracking of C fluxes into autotrophs and further into the microbial food web over time. Anoxic groundwater microcosms were spiked with ^{13}C-labeled CO_2 and thiosulfate, and as most SOB from the site possess genes for denitrification (Kumar et al., 2018), nitrate was added as electron acceptor. Autotrophic growth fueled by thiosulfate oxidation and denitrification has been described in various groundwater ecosystems including the Hainich CZE (Anantharaman et al., 2016; Kumar et al., 2018). Metabolic labeling was further combined with metagenomics and metaproteomics to provide insights into the metabolic versatility of groundwater SOB.

2. Material and methods

2.1. Field site description

Groundwater samples were collected in February 2019 at well H52 of the Hainich CZE located in the Hainich National park, Thuringia, Germany (Kohlhepp et al., 2017; Küsel et al., 2016). Well H52 reaches the upper aquifer assemblage in the Meissner formation of the Upper Muschelkalk (Middle Triassic), dominated by mudstone and limestone, in approximately 65 m depth. The groundwater of this fractured aquifer is characterized by anoxic conditions, a pH of 7.3 ± 0.1, dissolved organic C (DOC) concentrations around 1.0 mg/L, nitrate concentrations of 1.0 ± 4.0 mg/L, and sulfate concentrations of 90.0 ± 9.9 mg/L. Bicarbonate concentrations are at 397.0 ± 22.0 mg/L and CO_2 at 25.7 ± 6.1 mg/L (Lehmann and Totsche, 2020).

2.2. Groundwater sampling, microcosms setup, and chemical analysis

Groundwater was sampled in autoclaved 10 L glass bottles using a submersible pump (Grundfos MP1, Grundfos, Bjerringbro, Denmark) with a pump rate of 15.0 ± 1.0 L min^{-1}. To maintain anoxic conditions in these microcosms, the bottles were filled up to the edge avoiding air bubbles. Nitrogen was injected until the final water volume reached 8 L. As day 0 reference, water from three microcosms was directly filtered over 0.2-µm pore size polyethersulfone membrane supor® filters (PALL Corporation, Michigan, USA). The remaining 18 microcosms were incubated at constant 15 °C and darkness over 7, 21, and 42 days in controlled climate chambers (Johnson Controls, Cork, Ireland), mimicking the conditions in the original groundwater. To monitor anoxic conditions, SP-PSt3-YAU-D3-YOP sensor spots (PreSens, Regensburg, Germany) were added to one replicate microcosm of each timepoint and measured using the Fibox 4 detector (PreSens, Regensburg, Germany), ensuring dissolved oxygen concentrations below the detection limit of 0.03% throughout incubation. To stimulate SOB activity, 2.5 mM thiosulfate, and 200 µM nitrate and ammonium were added from sterile, anoxic stock solutions. After three weeks, another 200 µM nitrate was added to the remaining microcosms. For stable isotope probing experiments, triplicate incubations per timepoint were treated with 3.1 mM $Na^{13}CO_3$ (Cambridge isotope laboratories, Cambridge, UK) and 3.5 mM $^{13}CO_2$ (Sigma-Aldrich, St. Louis, USA), and further triplicates with the ^{12}C-equivalents. The amounts were chosen equal to the dissolved inorganic C (DIC) concentrations within the H52 groundwater, to achieve around 50% ^{13}C-DIC labeling. To monitor microbial activity during incubation, concentrations of nitrate, sulfate, and thiosulfate were determined twice per week using standard colorimetric procedures (Supplementary information).

2.3. Biomolecule extraction, quantitative PCR and amplicon sequencing

Replicate incubations were terminated after 7, 21, and 42 days by filtration as described above. Filters were stored at – 80 °C until combined DNA/protein extraction using a phenol-based approach as described (Taubert et al., 2018). Abundances of bacterial 16S rRNA genes, and of RuBisCO genes *cbbM* and *cbbL* were analyzed by qPCR using an Mx3000P instrument (Agilent, Böblingen, Germany) and the Maxima SYBR Green qPCR Mastermix (Thermo Fisher Scientific, Germany). Amplicon sequencing of the bacterial 16S rRNA gene was carried out on a MiSeq Illumina system using v3 chemistry (Illumina Inc., San Diego, USA). Sequence analysis was performed in Rv4.1.3 following the DADA2 SOP. Details on DNA and protein extraction, qPCR analysis and amplicon sequencing are provided in the supplementary information.

Amplicon sequence variants (ASVs) classified as *Sulfurimonas, Sulfuricella* and *Curvibacter* were filtered and screened against the ASV dataset of the Hainich CZE time series (Hermans et al*., in preparation*). Samples for the time series were collected on a monthly basis over eight consecutive years (2013–2021), filtered, extracted and sequenced as described elsewhere (Yan et al., 2021). ASV calling was performed as described before (Supplementary information). Relative abundances of *Sulfurimonas, Sulfuricella* and *Curvibacter* ASVs were summed per month, respectively. See Table S2 for all software and database sources.

2.4. Metagenomics analysis

To obtain genomes of the key organisms within the groundwater incubations, metagenomic sequencing was performed on DNA extracted from two selected microcosms, covering the last two timepoints and the majority of taxonomic diversity. DNA sizing, quantitation, integrity, and purity were determined using the Agilent 2100 Bioanalyzer system (Santa Clara, CA, USA). Library preparation was performed with an NEBNext Ultra II DNA Lib-Prep Kit (New England Biolabs, Ipswich, MA, USA), followed by multiplexed sequencing on one flow cell of an Illumina NextSeq 500 system (2 × 150 bp; Illumina, Inc., San Diego, CA, USA). Quality filtering of raw sequences and bin assembly, refinement, classification, and dereplication was done as described elsewhere (Taubert et al., 2022). Gene calling and functional annotation of gene sequences as well as translation into amino acid sequences for metaproteomics analysis was done using prokka v1.13.3. The final metagenome-assembled genomes (MAGs) were manually refined using Anvi'o v6.1. To investigate metabolic functions and assess pathway completeness, KEGG orthologs were assigned to gene sequences using KofamScan v2021–10–03 of KEGG-release 100.0. For quality filtering, the e-value was set below 0.01 and the score above threshold x0.8 or if

CORRECTED PROOF

no threshold was available above 100. Pathway completeness was assessed via KEGG decoder v1.3 and the online Reconstruct tool of KEGG Mapper V.5.0. Pathways of particulate interest were further investigated manually via NCBI-BLAST. Metagenomic and amplicon sequencing data are available at NCBI under BioProject accession PRJNA962518. See Table S2 for all software and database sources.

2.5. Metaproteomics analysis

Extracted proteins were purified by SDS-polyacrylamide gel-electrophoresis, cleaved by tryptic digestion of the 1D gel pieces and prepared for high-resolution mass spectrometry as described previously (Taubert et al., 2018). LC-MS/MS was performed on a Q-Exactive HF instrument (Thermo Fisher Scientific) equipped with a TriVersa NanoMate source (Advion Ltd., Harlow, UK) in LC chip coupling mode. Five microliters of peptide lysate were separated via an Ultimate 3000 nanoRSLC-system (Dionex/Thermo Fisher Scientific, Waltham, MA, USA). Raw data files were analyzed using the Sequest HT search algorithm in Proteome Discoverer™ Software Version 1.4.1.14 (Thermo Fisher Scientific, Waltham, MA, USA). For peptide identification, a custom-made database was constructed based on predicted amino acid sequences obtained from the previously constructed MAGs. Enzyme specificity was set to trypsin allowing two missed cleavages, precursor mass tolerance to 5 ppm, false discovery rate to 0.01, fragment mass tolerance to 0.05 Da, and methionine oxidation and cysteine carbamidomethylation were selected as modifications. Functional and taxonomic classification was based on gene annotations of the MAGs. Mass spectrometry proteomics data have been deposited into the ProteomeXchange Consortium via the PRIDE partner repository with the dataset identifier PXD04038.

2.6. Stable isotope cluster analysis

MS-Data from ^{12}C-samples was used to identify isotopologue patterns of classified peptides in mass spectra of the ^{13}C-labeled samples, yielding peak lists manually selected using the Xcalibur Qual-Browser v.2.0.7 (Thermo Fisher Scientific, Waltham, MA, USA). Quantification of ^{13}C-incorporation in identified peptides and relative ^{13}C-isotope abundances (RIA) calculation was done by comparing peptide masses, chromatographic retention times and MS/MS-fragmentation patterns as described previously (Taubert et al., 2012). Only MS-signals with mass deviation below 10 ppm and retention time deviation below 3 min were selected and only unique peptides with a peak area of 10^8 or higher were included in the quantification. For verification, isotopologue patterns were manually compared between replicates, and patterns with overlapping signals of other peptides were excluded. MAGs with a minimum of three peptides identified at all three timepoints were selected for SIsCA. A total of 674 isotopologue patterns were included in the analysis. SIsCA was done in Rv3.6.2 using the vegan software package for PCA analysis and ggplot2 for data visualization as described previously (Taubert et al., 2022). To estimate CO_2-incorporation into microbial biomass C, relative MAG abundances over time were calculated based on their total peptide counts per timepoint, multiplied with the respective RIA, and averaged over the whole community, or per SIsCA cluster. As 50% ^{13}C-incorporation corresponds to 100% labeling in our study, values were extrapolated accordingly to estimate the total CO_2 uptake.

3. Results

3.1. Thiosulfate oxidation and nitrate reduction fueled rapid microbial growth

All groundwater microcosms responded rapidly to addition of thiosulfate and nitrate, with bacterial abundances increasing by two orders of magnitude from $3.03 \bullet 10^7 \pm 2.12 \bullet 10^7$ at the start of incubation to $3.93 \bullet 10^9 \pm 3.66 \bullet 10^9$ 16S rRNA gene copies per L groundwater after six weeks (mean ± stdev, $p = 0.048$, Student's t-test, Fig. S1). The strongest growth was observed in the first week, with no significant increase in 16S rRNA gene copy numbers towards the third and sixth week (7 to 21 days: $p = 0.076$, 7 to 42 days: $p = 0.13$). Nitrate concentrations initially decreased by -8.32 ± 1.54 μmol L^{-1} d^{-1} (slope of linear regression ± standard error), leading to complete depletion after 25 days (Fig. S2). After the second amendment with nitrate, a similar decrease of -8.88 ± 0.61 μmol L^{-1} d^{-1} occurred. Thiosulfate and sulfate concentrations remained stable early on, but between day 21 and 42, thiosulfate decreased by -11.8 ± 6.48 μmol L^{-1} d^{-1}, and sulfate increased by 17.85 ± 7.37 μmol L^{-1} d^{-1}. Stoichiometrically, the ratio of nitrate: thiosulfate: sulfate over the whole incubation time was 1.4: 1: 1.5, close to the theoretical ratio of 1.6: 1: 2 for nitrate-dependent thiosulfate oxidation but with a slightly lower production of sulfate than expected. Overall, the increase in biomass together with observed changes in hydrochemistry suggested thiosulfate oxidation linked to nitrate reduction as driving force for microbial growth in the microcosms.

3.2. Sulfurimonas, Sulfuricella and Curvibacter species dominated throughout the incubation period

The microbial community composition in all groundwater microcosms shifted strongly from day 0 to day 7 ($p = 4.12 \bullet 10^{-38}$, two-factor ANOVA), without further changes thereafter (7 to 21 days: $p = 0.21$, 21 to 42 days: $p = 0.26$, two-factor ANOVA). Three genera accounted for the majority of the community: the *Campilobacterota Sulfurimonas* (56.3%, mean of 16S gene reads over all time points, Figs. 1, S4) and the *Gammaproteobacteria Sulfuricella* (13.8%) and *Curvibacter* (6.7%). *Gammaproteobacteria* further comprised *Sulfuritalea* (1.2%), *Hydrogenophaga* (0.8%), *Thiobacillus* (0.6%), and other *Burkholderiales*. Major abundant taxa in the untreated groundwater, like *Cand.* Paceibacteria (42.0%), *Thermodesulfovibrionia* (12.2%), and *Cand.* Brocadiae (4.8%), decreased during incubation to 1.3%, 0.4%, and 0.01%, respectively.

Metagenomics yielded 183 MAGs, including 3 MAGs of *Campilobacterota* and 53 MAGs of *Gammaproteobacteria. Sulfurimonas* and *Sulfuricella* were represented by one high-quality MAG each (Table S3), and for *Curvibacter,* two distinct MAGs were recovered (Average nucleotide identity: 91%). Further MAGs belonged to *Alphaproteobacteria* (3 MAGs) and *Bacteroidia* (6 MAGs), as well as *Cand.* Paceibacteria (34 MAGs), *Cand.* Brocadiae (4 MAGs), and *Thermodesulfovibrionia* (4 MAGs). MAG-resolved metaproteomics resulted in 104,930 classified peptides, with 24,459 belonging to *Sulfurimonas* MAG_154, 13,145 to *Sulfuricella* MAG_156, and 7746 to *Curvibacter* MAG_60 or MAG_85 (Fig. S5). Their combined contribution of 43.2% on protein level and 76.8% on 16S level suggested a key importance of these three genera among the groundwater SOB community.

3.3. SIsCA revealed CO_2 as major C source

After only seven days, 90.2% of the microbial biomass C was derived from CO_2, corresponding to an average daily replacement of 12.9% of microbial biomass C, and after 42 days this value increased slightly to 97.2%. This indicated chemolithoautotrophic CO_2 fixation as the main C source in the microcosms. SIsCA revealed four clusters of organisms with distinct ^{13}C-incorporation patterns, covering 26 MAGs of six bacterial phyla (Fig. 2, Table S3). Cluster I showed a consistent ^{13}C-incorporation of 44.0 ± 2.0% (mean ± stdev) over all timepoints, corresponding to complete labeling and roughly 98% CO_2-incorporation within the context of our experiment. This indicated strict autotrophic growth via CO_2 fixation. In addition to *Sulfurimonas* MAG_154 and *Sulfuricella* MAG_156, the cluster contained 10 MAGs belonging e.g. to *Sulfuricurvum* (*Campilobacterales*), *Sulfuritalea, Hydrogenophaga*, and

CORRECTED PROOF

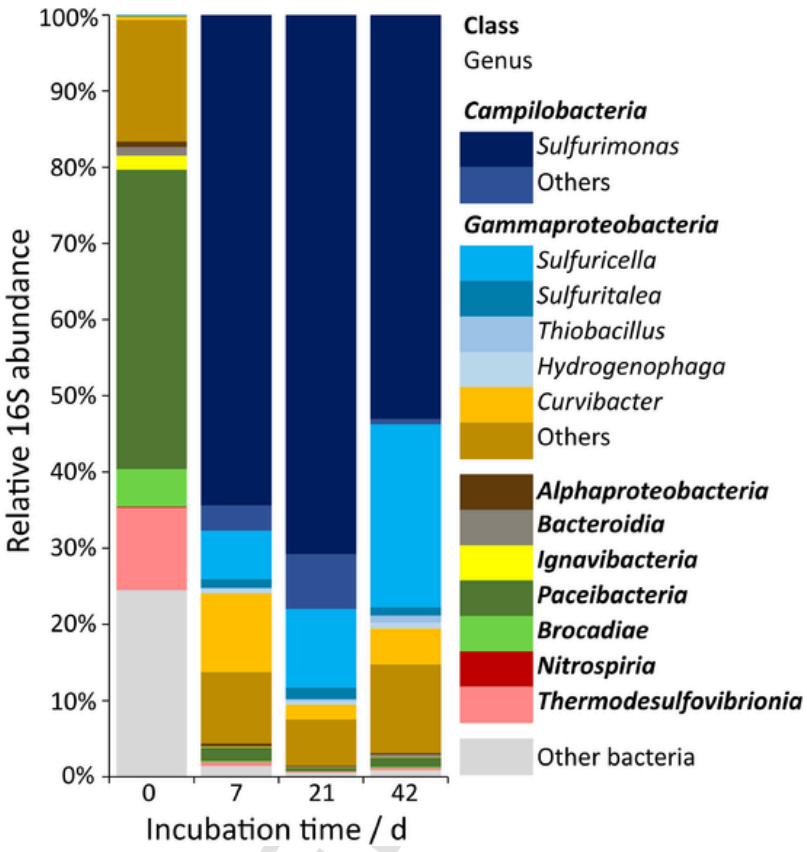

Fig. 1. Composition of the microbial community in the groundwater microcosms. Bar plots represent the relative 16S abundance of bacterial groups in the original groundwater (0 days) and after 7, 21, and 42 days of incubation with reduced S amendment. 16S numbers were averaged for replicate samples. 'Others' include all members of the respective Class not specified in listed Genera. 'Other bacteria' includes all classes < 1% relative abundance.

Thiobacillus (*Burkholderiales*). Altogether, cluster I MAGs represented 61.7% of all peptides, accounting for most of the CO_2 fixation in the microcosms.

Cluster II increased in ^{13}C-incorporation from 16.7 ± 9.8% after 7 days to 25.9 ± 9.2% after 21 days and 40.1 ± 3.2% after 42 days (mean ± stdev; $p = 5.77 \cdot 10^{-6}$ and $1.28 \cdot 10^{-5}$, respectively, Student's *t*-test, Fig. S6). These incorporation patterns indicated initial growth on organic C, either from chemolithoautotrophic primary production or the groundwater DOC pool, and CO_2 fixation later on, suggesting a mixotrophic lifestyle. In addition to both *Curvibacter*, cluster II contained MAGs affiliated with *Dechloromonas, Polaromonas* and *Caulobacter*. Combined cluster II MAGs accounted for 11.47% of all peptides.

The last two clusters contained eight MAGs, three in cluster III belonging to *Polaromonas, Prolixibacteraceae*, and *Cand.* Paceibacteria, and five in cluster IV classified as *Cand.* Brocadiae, *Cand.* Paceibacteria, and *Nitrospiria*. Cluster III MAGs displayed a moderate ^{13}C-incorporation of 15.3 ± 4.6% (mean ± stdev) over all timepoints. This labeling either originated from cross-feeding on ^{13}C-labeled organic compounds from chemolithoautotrophic primary production in addition to groundwater DOC or to some extent anaplerotic uptake of ^{13}C-labelled CO_2. Cluster IV MAGs lacked any label incorporation, indicating inactivity. Combined, these eight MAGs accounted for 2.78% of all peptides, representing only a small proportion of the microbial community in the groundwater microcosms.

3.4. *Sulfurimonas, Sulfuricella and Curvibacter used different metabolic strategies*

For thiosulfate oxidation, *Sulfurimonas* and both *Curvibacter* MAGs expressed the full Sox system consisting of *soxCDYZAXB* for complete oxidation to sulfate via the Kelly-Friedrich-pathway (Fig. 3,(Friedrich et al., 2001; Kelly et al., 1982). In contrast, *Sulfuricella* contained a truncated *soxYZAXB* gene cluster, lacking sulfur dehydrogenase genes *soxCD*. Instead, another S oxidation system including *dsrAB, aprAB* and *sat* was present. Absence of *dsrD*, encoding an allosteric activator of DsrAB during sulfite reduction (Ferreira et al., 2022), and presence of sulfurtransferase DsrEFH suggested S oxidation by this pathway (Ghosh and Dam, 2009). These pathways were also represented in the proteomes of the organisms. Furthermore, all four organisms translated enzymes involved in (poly)sulfide oxidation including sulfide:quinone reductase (Sqr) and, in *Sulfuricella* and *Curvibacter*, flavocytochrome-c-sulfide dehydrogenase (Fcc). Interestingly, *sqr* types II, IV and VI, adapted to different sulfide concentrations, were encoded in *Sulfurimonas* MAG_154, while the other three MAGs featured only high-affinity *sqr* type I (Fig. S7). *Sulfurimonas* and *Sulfuricella* further contained hydrogenases in their genomes, enabling H_2 as an alternative energy source. Both organisms produced proteins for several periplasmic hydrogenases and the cytoplasmic hydrogenase complex HoxS. In the *Curvibacter* MAGs, hydrogenase genes were absent, representing a distinct difference in metabolic abilities of cluster I autotrophs and cluster II mixotrophs.

As a second difference, *Sulfurimonas* and *Sulfuricella* featured enzymes for complete nitrate reduction to nitrogen gas, including either cytoplasmic or periplasmic nitrate reductases (Nap and Nar, respectively), nitrite reductase (Nir), nitric oxide reductase (Nor), and nitrous oxide reductase (Nos). Additionally, they featured polysulfide reductase complex Psr and *Sulfuricella* contained a selenite, a tetrathionate and a DMSO reductase, signifying a high flexibility regarding their respiratory electron acceptors. In contrast, *Curvibacter* MAGs produced only a soluble nitrate reductase (Nar) for nitrate reduction to nitrite, yielding less energy compared to the full reduction.

CORRECTED

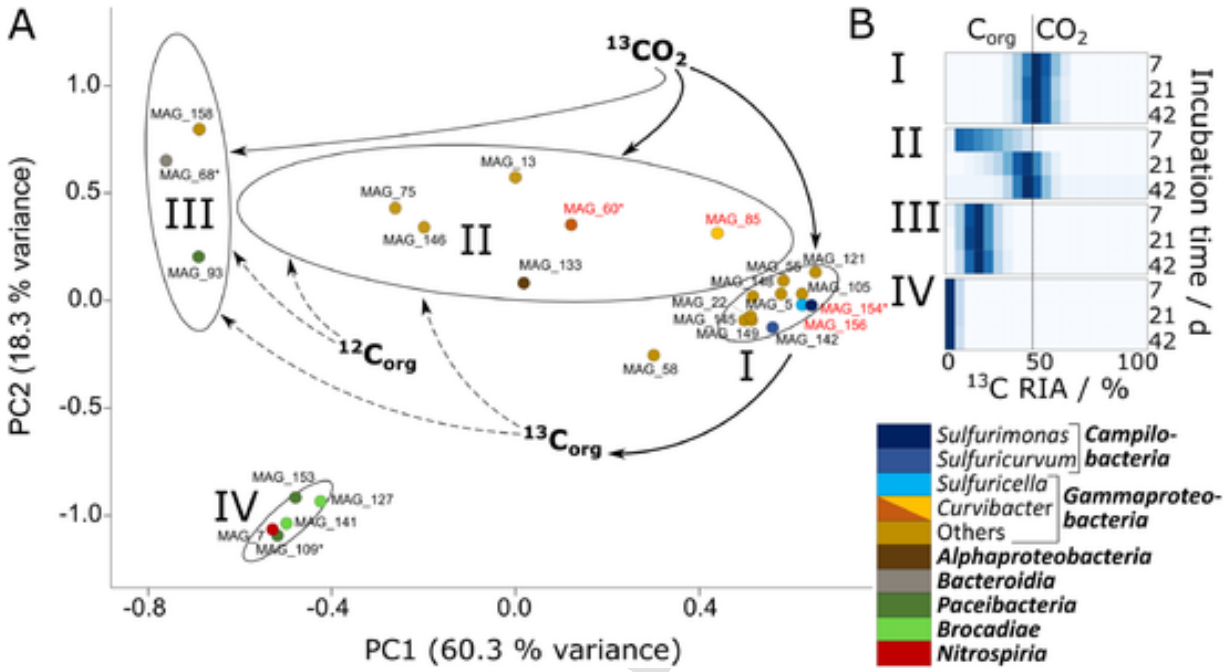

Fig. 2. Clustering of selected MAGs based on C consumption. A SIsCA based on ^{13}C-incorporation profiles over 7, 21, and 42 days of incubation obtained from SIP-metaproteomics. Each point in the PCA represents one MAG colored according to its taxonomic affiliation. Clusters are numbered from I - IV, and framed by ellipses based on 90% confidence intervals. Arrows indicate the C flux between clusters. B ^{13}C-incorporation profiles over time of one representative MAG per cluster. Heatmaps show the incorporation of ^{13}C into the peptides of the respective MAG after 7, 21, and 42 days of incubation (5% intervals, ranging from 0 to 100% ^{13}C relative isotope abundance, RIA). Asterisks indicate MAGs corresponding to the heatmaps. MAGs affiliated with *Sulfurimonas, Sulfuricella,* and *Curvibacter* are marked in red.

For C assimilation, *Sulfuricella* and *Curvibacter* contained and expressed the full CBB cycle including *cbbM* encoding RuBisCO type II. *Sulfurimonas* contained all genes of the rTCA cycle including *aclAB* encoding ATP citrate lyase (ACL). The production of respective peptides, including key enzyme ACL, indicated the use of this pathway for CO_2 fixation. Interestingly, only *Curvibacter* MAGs featured various pathways for the degradation of complex organic compounds like fatty acids, amino acids, and aromatics. This comprised proteins for beta oxidation including acyl-CoA dehydrogenase (Acd), enoyl-CoA hydratase (PaaF), 3-hydroxyacyl-CoA dehydrogenase (FadN), and acetyl-CoA acyltransferase (FadJ). Aromatic C degradation abilities included alternative routes for benzoate degradation, tyrosine and phenylalanine catabolism, and the oxidation of vanillin and terephthalate in both MAGs (Fig. S8, Supplementary information). *Curvibacter* MAGs also produced a broader array of transport proteins, for amino acid import, other carboxylic acids, and organic sugars, compared to *Sulfurimonas* and *Sulfuricella*. Observed differences in their C acquisition modules hence matched the C assimilation strategies determined by SIsCA for the cluster I and II organisms.

3.5. Metabolic versatility goes beyond cluster distinction

Extending the analysis to all SIsCA MAGs showed that the truncated Sox plus Dsr system was a common feature of the gammaproteobacterial members in cluster I (Fig. 4). In contrast, most MAGs of cluster II expressed the full Sox system like *Curvibacter*. As exceptions, both *Hydrogenophaga* of cluster I employed the full Sox system, while cluster II member *Hydrogenophilaceae* MAG_146 possessed the truncated Sox plus Dsr system, and *Sulfuricurvum* of cluster I had only *soxXAYZB*. The ability to oxidize sulfide was shared by all MAGs of cluster I and II, with 17 out of 18 producing proteins for Sqr or Fcc.

Hydrogenase genes were present in all cluster I MAGs, and gene products were detected for six of them. In addition to periplasmic hydrogenases (Hya, Hyb or Hyd), all cluster I MAGs except *Hydrogenophaga* MAG_55 featured cytoplasmic hydrogenases (Hox, Hyf or Ech). In cluster II, periplasmic hydrogenase genes were only found in three MAGs, and two produced respective proteins, while cytoplasmic hydrogenase genes were present in two MAGs, without detected proteins.

The full pathway for denitrification was present in seven additional cluster I members including *Sulfuritalea* MAG_121, *Hydrogenophaga* MAG_55, and two *Thiobacillus* MAGs. The absence of downstream denitrification enzymes as in *Curvibacter* was not observed in the other cluster II members, but none of the MAGs contained the complete pathway, and *Dechloromonas* MAG_13 employed periplasmic nitrate reductase Nap instead of cytoplasmic Nar. Additionally, alternative pathways for anaerobic respiration in cluster I indicated a greater flexibility in electron donors than in cluster II (Supplementary information).

For CO_2 fixation, all *Gammaproteobacteria* in cluster I and II featured the full CBB cycle, while the *Campilobacterota* employed the rTCA pathway (Table S5). Matching the shift towards higher CO_2 assimilation of the cluster II microbes, relative numbers of RuBisCO peptides increased from initial 0.43 ± 0.07% to 0.98 ± 0.17% at day 42 ($p = 0.02$, Student's *t*-test, Fig. S9). The *Alphaproteobacterium Caulobacter* MAG_133 in cluster II was the only organism lacking any CO_2 fixation pathway, suggesting labeling by cross-feeding on primarily produced C. Routes for the degradation of complex organic compounds were absent in almost all cluster I MAGs, apart from central C metabolism like glycolysis and the TCA cycle. In contrast, all members of cluster II featured catabolic routes for fatty acids and aromatics, including beta oxidation and pathways for phenylalanine and tyrosine degradation. Furthermore, proteins for the import of amino acids, carboxylic acids, lipids, and carbohydrates were produced by all cluster II members. Interestingly, cluster I members *Sulfuritalea* MAG_121 and *Hydrogenophaga* MAG_5 and MAG_55 represented exceptions, featuring complete pathways for fatty acid and aromatic amino acid degradation in genomes and proteomes. In general, meta'omics confirmed autotrophy of cluster I and mixotrophy of cluster II microbes, but the presence of potential mixotrophs in

CORRECTED

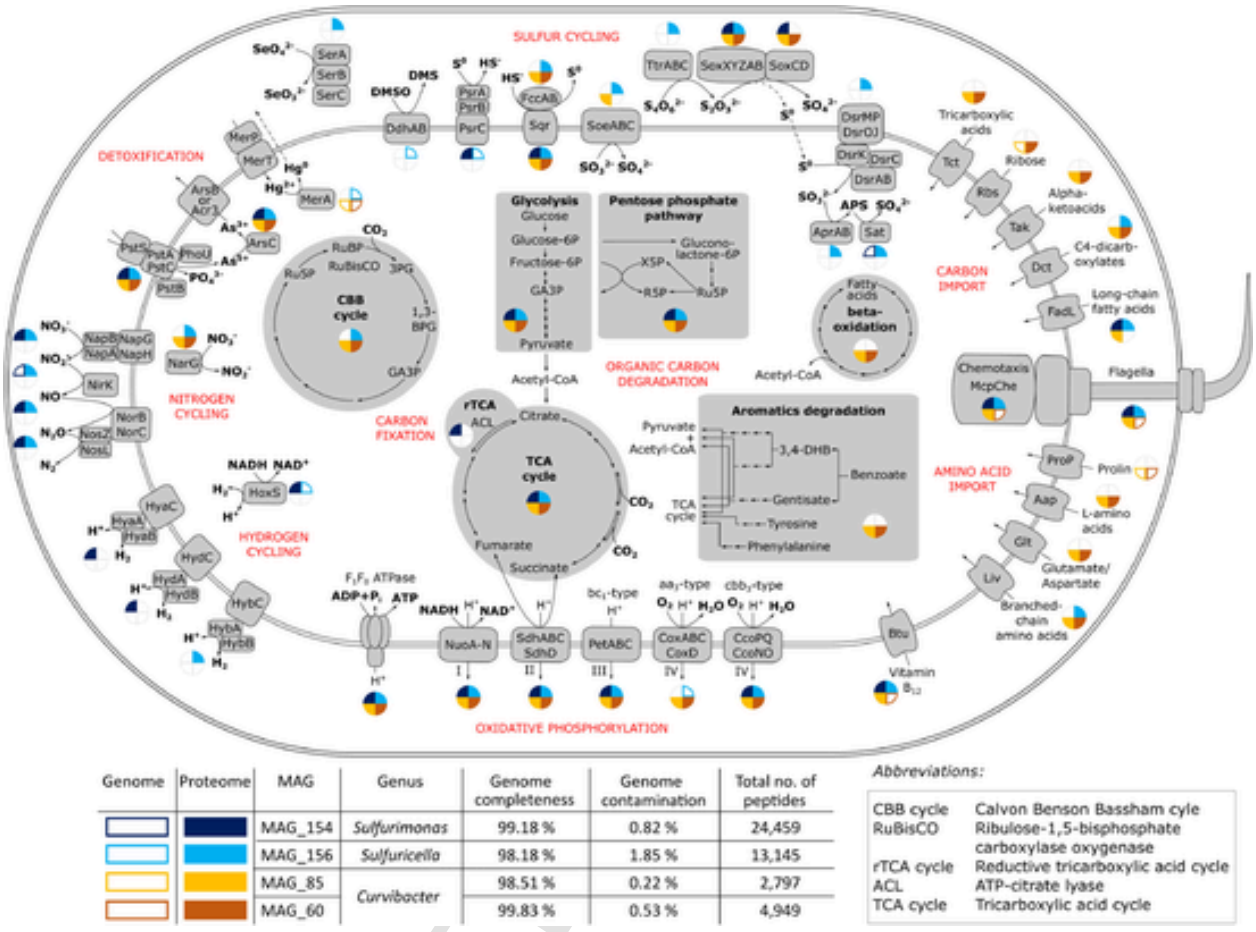

Fig. 3. Metabolic map of *Sulfurimonas* MAG_154, *Sulfuricella* MAG_156, and *Curvibacter* MAG_85, and MAG_60. MAGs represent cluster I (MAG_154 + 156) and cluster II (MAG_85 + 60) of SIsCA. Pie charts next to each feature represent the presence in the genome (empty) or genome + proteome (filled) of the four selected MAGs (color key). Pie charts without specified protein names refer to the whole pathway. A full list of abbreviations is given in Table S4.

cluster I and a strict heterotroph in cluster II suggested a greater variety in survival strategies of SOB in the aquifer.

3.6. Sulfurimonas, Sulfuricella and Curvibacter were commonly present in anoxic and oxic groundwaters

To assess the importance of the four key players in the environment, we tracked their abundance in the Hainich CZE using *in situ* datasets covering eight years. All three genera were consistently present in anoxic and oxic groundwaters, typically with an abundance below 1% (Fig. S10). Interestingly, short-term increases in abundance could be observed several times: For example, *Sulfurimonas* accounted for 15.2% of the microbial community in an anoxic groundwater well in December 2015, and all three genera combined accounted for 12.9% in an oxic (5.1 ± 1.7 mg/L dissolved oxygen,(Lehmann and Totsche, 2020) groundwater well in September 2018. These sudden blooms suggested strong contributions of SOB to chemolithoautotrophic primary production. The occurrence of key players of our strictly anoxic microcosms in oxic groundwater further matched observations that sixteen cluster I and II MAGs produced proteins for aerobic respiration, and all possessed respective genes (Fig. 4). Among the four key players, all produced proteins for cbb3-type cytochrome-c oxidase Cco, known to work under low oxygen concentrations (Fig. 3,(Pitcher and Watmough, 2004). *Sulfuricella* and *Curvibacter* MAGs further contained genes for cytochrome-c oxidase Cox typical for aerobic conditions, without proteins detected. Being a facultative anaerobe hence might be another trait benefitting the survival of SOB in pristine groundwater.

4. Discussion

More than 90% of the total microbial biomass C was replaced by CO_2 fixation within the first week of incubation, showing the rapid response of the SOB community in our anoxic groundwater microcosms. Chemolithoautotrophs of cluster I accounted for two thirds of the microbial community on genomic and proteomic level, and included SOB abundant in the native groundwater, highlighting their potential for high activity and rapid growth. These organisms replaced 12.9% of microbial biomass C in the microcosms with CO_2-derived C per day, a 27-fold higher rate than the previously reported 0.47% of biomass C replaced per day *in situ* (Overholt et al., 2022). Considering the tenfold lower relative abundance of SOB in the groundwater well (Overholt et al., 2022) as compared to our microcosms, our findings show a similar CO_2 fixation activity. S-fueled primary production can thus explain the previously observed high assimilation of CO_2 into microbial biomass at the site (Overholt et al., 2022), supporting our first hypothesis. The second largest group of active microbes in the microcosms consisted of hetero- and mixotrophs, which incorporated 37% CO_2-derived C within the first week. The labeling patterns of these organisms suggested the partial assimilation of autotrophically produced organic compounds, verifying our second hypothesis. For cluster II mixotrophs, the increase in ^{13}C-labeling together with the increase in RuBisCO peptides over time suggested an initial uptake of autotrophically produced compounds followed by a shift towards CO_2 fixation. This led to a further increase in microbial biomass labeling towards 97% after 42 days and showed that not only autotrophic but also mixotrophic SOB contributed to CO_2 fixation.

CORRECT

Fig. 4. Functional profiling of active MAGs. Bubble sizes correspond to the total number of peptides per MAG and functional category over all timepoints. Asterisks indicate the presence of genes within the respective MAG belonging to the addressed metabolic feature if no peptides were identified. MAGs are divided according to their SIsCA cluster affiliation (I to IV). RuBisCO: Ribulose-1,5-bisphosphate carboxylase oxygenase, CBB: Calvin Benson Bassham cycle, (r)TCA: (reductive) tricarboxylic acid cycle, ACL: ATP-citrate lyase, WLP: Wood-Ljungdahl pathway, 3-HP: 3-Hydroxypropionate bicycle, 4-HB/ 3-HP: 4-Hydroxybutyrate/ 3-Hydroxypropionate cycle, Cyt c: Cytochrome c.

Mixing and matching of traits from C, S, N, and H_2 metabolism yielded six strategies of our SOB to adapt to different niches in the groundwater (Fig. 5). As a first trait, chemolithoautotrophic MAGs of cluster I related to *Sulfuricella, Thiobacillus, Sulfuritalea* and *Sulfuricurvum* contained a truncated Sox system. Lack of sulfane dehydrogenase SoxCD leads to incomplete thiosulfate oxidation to elemental S, which forms polysulfide structures like granules either stored in the periplasm or on the outer cell membrane (Welte et al., 2009). The formation of periplasmic granules has been shown for many *Gammaproteobacteria* (Maki, 2013; Welte et al., 2009), including *Thiobacillus* sp. (Boden et al., 2017; Katayama-Fujimura et al., 1984), while S storage on the outer cell membrane was found in *Sulfuricurvum kujiense* (Cron et al., 2019). Storage of thiosulfate-derived S might also explain the low amount of sulfate produced over the incubation period. Being in an intermediate redox state, S granules can provide both a substrate for anaerobic respiration and electrons for lithotrophic S oxidation. *Sulfuricella* and *Sulfuritalea* contained polysulfide reductases, enabling them to respire S as an alternative to nitrate. For oxidation, *Sulfuricella, Sulfuritalea* and *Thiobacillus* MAGs harbored the reversed Dsr-system (Ghosh and Dam, 2009). Using a single compound as a backup for respiration and chemolithotrophic energy production might significantly increase the fitness of microbes especially when the supply of S is not constant.

Alternative to energy storage, cluster II microbes like *Curvibacter, Polaromonas, Dechloromonas,* and *Caulobacter* used organic C. These MAGs produced enzymes involved in aromatics or fatty acid degradation, suggesting the usage of aromatic amino acids or lipids produced by the autotrophs for mixo- and heterotrophic growth. Such compounds are released by many bacteria and contribute to the formation of metabolic networks in natural environments (D'Souza et al., 2018; Pande and Kost, 2017). Incomplete labeling of these MAGs also indicated the uptake of unlabeled organic compounds. As no organic carbon was added in our experiment, this can only be derived from the low (1.0 mg/L) DOC concentrations in the groundwater (Lehmann and Totsche, 2020). Interestingly, *Hydrogenophaga* and *Sulfuritalea* MAGs also produced proteins for fatty acid and aromatics degradation, suggesting the potential for mixotrophic growth, although SIsCA depicted exclusive CO_2 fixation. The constitutive production of these enzymes might be explained by a higher cost for gene regulation compared to maintenance (Geisel, 2011), or by a shift towards exclusive growth on CO_2 already within the first week of incubation.

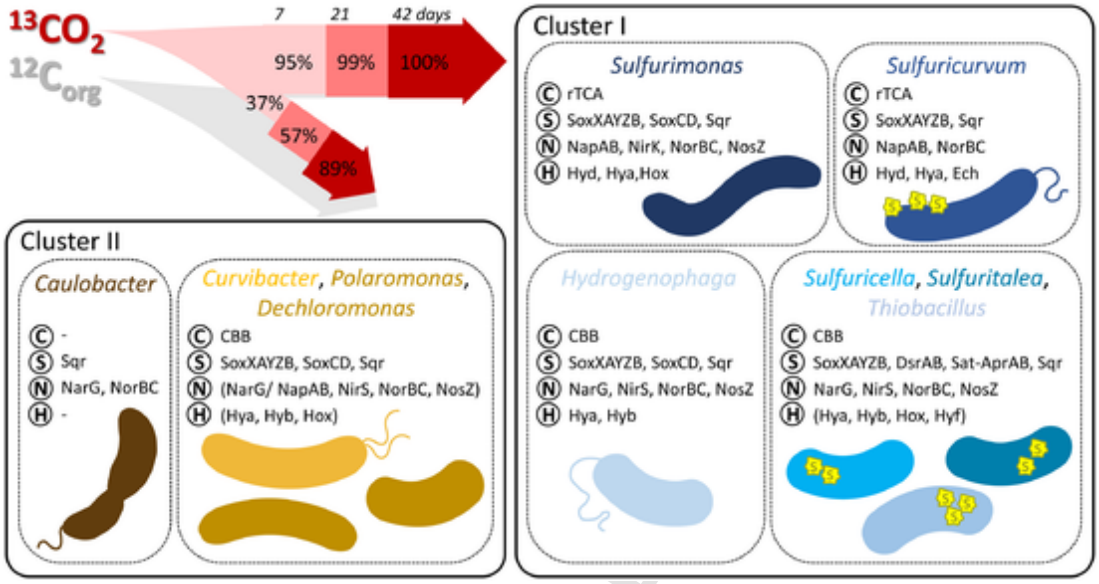

Fig. 5. Trait-based adaptation strategies of SOB in anoxic groundwater. Percentages are the amount of microbial C derived from CO_2 fixation after 7, 21, and 42 days. Cluster division is based on SIsCA. Brackets indicate that the included functions were only partially present in the respective microbes. Yellow cookies represent potential S storage globules. rTCA: reductive tricarboxylic acid cycle. CBB: Calvin-Benson-Bassam cycle.

A third trait, found in most cluster I autotrophs, was efficient nitrate respiration by a complete denitrification pathway. Complete oxidation of 1 mol thiosulfate to sulfate requires 1.6 mol nitrate if fully reduced to nitrogen gas (Matějů et al., 1992), but partial denitrification e.g. to nitrite requires 4 mol of nitrate per mol thiosulfate. Furthermore, cytoplasmic nitrate reductase Nar translocates more protons per respired nitrate than periplasmic Nap (Chen and Strous, 2013; Stewart et al., 2002), resulting in higher ATP production. Especially for autotrophs, efficient denitrification can therefore be crucial as CO_2 fixation is costly (Zhao et al., 2021). In comparison, all cluster II MAGs expressed less efficient routes for nitrate respiration, containing either a truncated denitrification pathway, like *Curvibacter*, or using the periplasmic system, like *Dechloromonas*. For mixo- and heterotrophs, this might be no disadvantage as they can satisfy their metabolic needs with groundwater DOC avoiding costly CO_2 fixation. Our study further demonstrated anaerobic growth of *Caulobacter* MAG_133, potentially via reduced S oxidation coupled to nitrate respiration. *Caulobacter* sp. typically grow aerobically, and anaerobic growth has only been described in the context of cellulose fermentation (Song et al., 2013). The potential for chemolithotrophic growth on reduced S and nitrate could be an adaptation of *Caulobacter* to the fluctuating redox conditions in groundwater environments.

All chemolithoautotrophic and even some mixotrophic groundwater SOB produced a variety of hydrogenases, providing an alternative energy source for chemolithotrophic growth. H_2 is commonly produced by fermenters or nitrogen-fixing microorganisms (Das and Veziroğlu, 2001), both present in the Hainich aquifers (Kumar et al., 2018; Wegner et al., 2019). While periplasmic hydrogenases are involved in hydrogen-dependent growth, soluble cytoplasmic hydrogenases have been proposed to replenish the pool of oxidized ferredoxin to run the TCA cycle non-reductively and degrade internal C stores under energy starvation in members of the *Campilobacterota* including *Sulfurimonas* sp. (Campbell et al., 2006; Han and Perner, 2015). Cytoplasmic hydrogenases were produced by *Sulfurimonas* MAG_154 and most cluster I autotrophs, indicating the degradation of internal C stores via the TCA cycle as a potential way to withstand reduced S limitations.

Lastly, both *Campilobacterota* MAGs performed CO_2 fixation via the rTCA cycle, which requires only a third of the ATP per CO_2 compared to the CBB cycle of the *gammaproteobacterial* MAGs (Zhao et al., 2021). This might have enabled the *Campilobacterotas* to grow exclusively on CO_2 despite the lower efficiency of their Nap-mediated denitrification. Furthermore, the full Sox system present in *Sulfurimonas* was shown to allow faster growth under rapid consumption of reduced S, compared to the truncated Sox/ reverse Dsr system (Klatt and Polerecky, 2015). *Sulfurimonas* further contained type VI Sqr known to be efficient at high sulfide concentrations above 4 mM (Marcia et al., 2010). The organism hence seems to be ideally endowed to rapidly respond to temporal exposure to higher levels of reduced S. Blooms of *Sulfurimonas* observed on several occasions over the eight-year period could thus rapidly remove compounds like hydrogen sulfide and bolster CO_2 fixation within the aquifer. Due to their rapid response, *Sulfurimonas sp*. may be valuable not only for the removal of reduced S compounds, but also for nitrate remediation in groundwater ecosystems, as shown in a study using pyrite minerals to stimulate denitrifying SOB in a nitrate-contaminated aquifer (Pu et al., 2014). Furthermore, thiosulfate-stimulated groundwater enrichments could provide a suitable community and sufficient biomass to set up bioreactors for wastewater treatment (e.g.(Sierra-Alvarez et al. 2007).

Traits allowing SOB to switch between autotrophy and heterotrophy, rapidly respond to high S concentrations and withstand limitations provides them access to various ecological niches. Especially organisms able to store S compounds like *Sulfuricella* and *Sulfuritalea* compose core species of the groundwater microbiome at the site (Herrmann et al., 2015). Other abundant SOB related to *Sulfurifustaceae* and *Acidiferrobacteraceae* also expressed genes for potential S storage via the truncated Sox/reverse Dsr system (Overholt et al., 2022; Wegner et al., 2019), showing the importance of this trait in the oligotrophic aquifer. Traits like internal S storage or H_2 oxidation were further reported for many S-oxidizing chemolithoautotrophs in oligotrophic habitats like marine ecosystems (Anantharaman et al., 2013; Bazylinski et al., 2004; Schwedt et al., 2012; Shah et al., 2019). SOB like *Thiobacillus* and *Sulfuricurvum,* less abundant in the shallow Hainich groundwater but active in the microcosms, dominated autotrophic communities in subglacial lakes or deep crystalline aquifers (Emerson et al., 2016; Marteinsson et al., 2013; Mikucki et al., 2016). It is hence not surprising that also in other (oligotrophic) anaerobic ecosystems like coastal marine sediments, more than half of all CO_2 fixation was attributed to SOB activity (Boschker et al., 2014; Dyksma et al., 2016).

In addition to SOB, anammox-performing *Cand.* Brocadiales MAGs were detected in our anoxic groundwater microcosms, but remained in-

active despite the addition of ammonium and the production of nitrite via incomplete denitrification. As micromolar concentrations of reduced S compounds like sulfide can inhibit anammox bacteria (Dapena-Mora et al., 2007; Jensen et al., 2008), growth of *Cand.* Brocadiales was probably hindered in our setup. *In situ*, SOB might play a role in removal of sulfide and hence promote anammox activity, as shown in a co-culture of anammox bacteria and *Sulfurimonas denitrificans* and suggested as one role of *Sulfurimonas* sp. in pelagic redox clines (Henkel et al., 2022; Russ et al., 2014).

Key SOB of our anoxic groundwater microcosms were also abundant in oxic groundwater with higher surface connectivity (Benk et al., 2019; Kohlhepp et al., 2017). Typically, N-oxidizers using surface-derived N compounds as energy source dominate primary production at this site (Overholt et al., 2022; Wegner et al., 2019), while SOB occur only in low abundance and primarily pursue a mixotrophic lifestyle (Taubert et al., 2022). However, several times during an eight-year period, blooms of autotrophic SOB were observed, reaching abundances of up to 13%. Fluctuations in groundwater recharge can cause changes in hydrochemical conditions (Benk et al., 2019) that might favor the activity of SOB. Reduced surface inputs would deprive N-oxidizers from their energy source and mixotrophs from organic C inputs, while SOB, utilizing autochthonously occurring reduced S, could prevail. Furthermore, higher levels of oxygen might enhance rock dissolution and release more reduced S (Kohlhepp et al., 2017), stimulating SOB activity. Accordingly, the interplay of organic C availability, surface N compounds, and oxygen with pyrite-rich bedrock can shape the activity of SOB and, more generally, govern chemolithoautotrophic primary production in groundwater habitats.

5. Conclusions

We were able to trace CO_2 fixation into the microbial groundwater food web and showed that S-fueled primary production can not only fuel hetero- and mixotrophic microbes but also dominate CO_2 fixation, replacing more than 90% of the microbial biomass within one week. *In situ*, key SOB of our microcosms composed up to 15% of the microbial community, highlighting the importance of geogenic S cycling for primary production in modern groundwater. This study also showed that to truly understand the impact of SOB on global biogeochemical cycles, detailed studies are necessary that go beyond omics to also unravel C fluxes. Affording the genes to realize traits like S storage, efficient denitrification, H oxidation, or rapid proliferation benefit SOB survival and increase their contribution to CO_2 fixation. The role of denitrification showed that not only presence, but also pathway completeness influences the efficiency of energy generation and should be considered in future studies. SOB might further boost the activity of anammox bacteria in aquatic habitats, removing potential inhibitors like sulfide and providing nitrite derived from incomplete denitrification for their growth. Furthermore, microbes that are efficient denitrifiers or that can respond rapidly to reduced S may be promising candidates for future nitrate or hydrogen sulfide groundwater remediation studies. This work significantly contributes to our understanding of the metabolic versatility among the groundwater SOB community, with each member contributing to a diverse pool of capabilities, and their major impact on CO_2 fixation in modern groundwater.

Supplementary information

Dataset S1
Dataset S2
Dataset S3

CRediT authorship contribution statement

Beatrix M. Heinze : Visualization, Methodology, Formal analysis, Data curation, Writing – review & editing. **Kirsten Küsel :** Writing – review & editing. **Nico Jehmlich :** Formal analysis, Writing – review & editing. **Martin von Bergen :** Formal analysis, Writing – review & editing. **Martin Taubert :** Visualization, Formal analysis, Data curation, Writing – review & editing.

Declaration of Competing Interest

The authors declare that they have no known competing financial interests or personal relationships that could have appeared to influence the work reported in this paper.

Data availability

Data will be made available on request.

Acknowledgements

We thank Falko Gutmann, Heiko Minkmar and Jens Wurlitzer for assistance in the field. We thank Ivonne Görlich and Marco Groth at the Core Facility DNA sequencing of the Leibniz Institute on Aging - Fritz Lipmann in Jena for help with the Illumina sequencing, and Will Overholt for advice during metagenomics analysis. We thank Syrie Hermanns for providing the time series data on the groundwater microbial community in the Hainich CZE. This work was supported financially by the Deutsche Forschungsgemeinschaft (DFG) via the Collaborative Research Centre AquaDiva (CRC 1076 AquaDiva Project-ID 218627073) of the Friedrich Schiller University Jena. MT gratefully acknowledges funding by the DFG under Germany´s Excellence Strategy, EXC 2051–Project-ID 390713860. Climate chambers and the infrastructure for Illumina MiSeq sequencing were financially supported by the Thüringer Ministerium für Wirtschaft, Wissenschaft und Digitale Gesellschaft (TMWWDG; project B 715-09075 and project 2016 FGI 0024 "BIODIV"). BH is grateful to the International Max Planck Research School for global Biogeochemical cycles (IMPRS-gBGC) for funding. MvB and NJ are grateful for funding of the UFZ for the ProMetheus platform for proteomics and metabolomics.

Supplementary materials

Supplementary material associated with this article can be found, in the online version, at doi:10.1016/j.watres.2023.120426.

References

Albertin, A.R., Sickman, J.O., Pinowska, A., Stevenson, R.J., 2012. Identification of nitrogen sources and transformations within karst springs using isotope tracers of nitrogen. Biogeochemistry 108 (1), 219–232.

Anantharaman, K., Breier, J.A., Sheik, C.S., Dick, G.J., 2013. Evidence for hydrogen oxidation and metabolic plasticity in widespread deep-sea sulfur-oxidizing bacteria. Proc. Natl. Acad. Sci. USA 110 (1), 330–335.

Anantharaman, K., Brown, C.T., Hug, L.A., Sharon, I., Castelle, C.J., Probst, A.J., Thomas, B.C., Singh, A., Wilkins, M.J., Karaoz, U., Brodie, E.L., Williams, K.H., Hubbard, S.S., Banfield, J.F., 2016. Thousands of microbial genomes shed light on interconnected biogeochemical processes in an aquifer system. Nat. Commun. 7 (1), 13219.

Bazylinski, D.A., Dean, A.J., Williams, T.J., Long, L.K., Middleton, S.L., Dubbels, B.L., 2004. Chemolithoautotrophy in the marine, magnetotactic bacterial strains MV-1 and MV-2. Arch. Microbiol. 182 (5), 373–387.

Bell, E., Lamminmäki, T., Alneberg, J., Andersson, A.F., Qian, C., Xiong, W., Hettich, R.L., Frutschi, M., Bernier-Latmani, R., 2020. Active sulfur cycling in the terrestrial deep subsurface. ISME J. 14 (5), 1260–1272.

Benk, S.A., Yan, L., Lehmann, R., Roth, V.N., Schwab, V.F., Totsche, K.U., Küsel, K., Gleixner, G., 2019. Fueling diversity in the subsurface: composition and age of dissolved organic matter in the critical zone. Front. Earth Sci. 7, 296.

Boden, R., Hutt, L.P., Rae, A.W., 2017. Reclassification of *Thiobacillus aquaesulis* (Wood & Kelly, 1995) as *Annwoodia aquaesulis* gen. nov., comb. nov., transfer of *Thiobacillus* (Beijerinck, 1904) from the Hydrogenophilales to the Nitrosomonadales, proposal of

CORRECTED PROOF

Hydrogenophilalia class. nov. within the 'Proteobacteria', and four new families within the orders Nitrosomonadales and Rhodocyclales. Int. J. Syst. Evol. Microbiol. 67 (5), 1191–1205.
Boschker, H.T., Vasquez-Cardenas, D., Bolhuis, H., Moerdijk-Poortvliet, T.W., Moodley, L., 2014. Chemoautotrophic carbon fixation rates and active bacterial communities in intertidal marine sediments. PLoS ONE 9 (7), e101443.
Campbell, B.J., Engel, A.S., Porter, M.L., Takai, K., 2006. The versatile ε-proteobacteria: key players in sulphidic habitats. Nat. Rev. Microbiol. 4 (6), 458–468.
Chen, J., Strous, M., 2013. Denitrification and aerobic respiration, hybrid electron transport chains and co-evolution. Biochim. Biophys. Acta Bioenerg. 1827 (2), 136–144.
Cron, B., Henri, P., Chan, C.S., Macalady, J.L., Cosmidis, J., 2019. Elemental sulfur formation by *Sulfuricurvum kujiense* is mediated by extracellular organic compounds. Front. Microbiol. 10, 2710.
D'Souza, G., Shitut, S., Preussger, D., Yousif, G., Waschina, S., Kost, C., 2018. Ecology and evolution of metabolic cross-feeding interactions in bacteria. Nat. Prod. Rep. 35 (5), 455–488.
Dapena-Mora, A., Fernández, I., Campos, J.L., Mosquera-Corral, A., Méndez, R., Jetten, M.S.M., 2007. Evaluation of activity and inhibition effects on Anammox process by batch tests based on the nitrogen gas production. Enzym. Microb. Technol. 40 (4), 859–865.
Das, D., Veziroğlu, T.N., 2001. Hydrogen production by biological processes: a survey of literature. Int. J. Hydrog. Energy 26 (1), 13–28.
Dyksma, S., Bischof, K., Fuchs, B.M., Hoffmann, K., Meier, D., Meyerdierks, A., Pjevac, P., Probandt, D., Richter, M., Stepanauskas, R., Mußmann, M., 2016. Ubiquitous Gammaproteobacteria dominate dark carbon fixation in coastal sediments. ISME J. 10 (8), 1939–1953.
Emerson, J.B., Thomas, B.C., Alvarez, W., Banfield, J.F., 2016. Metagenomic analysis of a high carbon dioxide subsurface microbial community populated by chemolithoautotrophs and bacteria and archaea from candidate phyla. Environ. Microbiol. 18 (6), 1686–1703.
Ferreira, D., Barbosa, A.C.C., Oliveira, G.P., Catarino, T., Venceslau, S.S., Pereira, I.A.C., 2022. The DsrD functional marker protein is an allosteric activator of the DsrAB dissimilatory sulfite reductase. Proc. Natl. Acad. Sci. USA 119 (4), e2118880119.
Friedrich, C.G., Rother, D., Bardischewsky, F., Quentmeier, A., Fischer, J., 2001. Oxidation of reduced inorganic sulfur compounds by bacteria: emergence of a common mechanism? Appl. Environ. Microbiol. 67 (7), 2873–2882.
Geisel, N., 2011. Constitutive versus responsive gene expression strategies for growth in changing environments. PLoS ONE 6 (11), e27033.
Ghosh, W., Dam, B., 2009. Biochemistry and molecular biology of lithotrophic sulfur oxidation by taxonomically and ecologically diverse bacteria and archaea. FEMS Microbiol. Rev. 33 (6), 999–1043.
Gleeson, T., Befus, K.M., Jasechko, S., Luijendijk, E., Cardenas, M.B., 2016. The global volume and distribution of modern groundwater. Nat. Geosci. 9 (2), 161–167.
Griebler, C., Lueders, T., 2009. Microbial biodiversity in groundwater ecosystems. Freshw. Biol. 54 (4), 649–677.
Han, Y., Perner, M., 2015. The globally widespread genus *Sulfurimonas*: versatile energy metabolisms and adaptations to redox clines. Front. Microbiol. 6, 989.
Hansel, C.M., Lentini, C.J., Tang, Y., Johnston, D.T., Wankel, S.D., Jardine, P.M., 2015. Dominance of sulfur-fueled iron oxide reduction in low-sulfate freshwater sediments. ISME J. 9 (11), 2400–2412.
Henkel, J.V., Schulz-Vogt, H.N., Dellwig, O., Pollehne, F., Schott, T., Meeske, C., Beier, S., Jürgens, K., 2022. Biological manganese-dependent sulfide oxidation impacts elemental gradients in redox-stratified systems: indications from the Black Sea water column. ISME J. 16 (6), 1523–1533.
Herrmann, M., Rusznyák, A., Akob, D.M., Schulze, I., Opitz, S., Totsche, K.U., Küsel, K., 2015. Large fractions of CO_2-fixing microorganisms in pristine limestone aquifers appear to be involved in the oxidation of reduced sulfur and nitrogen compounds. Appl. Environ. Microbiol. 81 (7), 2384–2394.
Jensen, M.M., Kuypers, M.M.M., Gaute, L., Thamdrup, B., 2008. Rates and regulation of anaerobic ammonium oxidation and denitrification in the Black Sea. Limnol. Oceanogr. 53 (1), 23–36.
Jewell, T.N., Karaoz, U., Brodie, E.L., Williams, K.H., Beller, H.R., 2016. Metatranscriptomic evidence of pervasive and diverse chemolithoautotrophy relevant to C, S, N and Fe cycling in a shallow alluvial aquifer. ISME J. 10 (9), 2106–2117.
Katayama-Fujimura, Y., Tsuzaki, N., Hirata, A., Kuraishi, H., 1984. Polyhedral inclusion bodies (carboxysomes) in *Thiobacillus* species with reference to the taxonomy of the genus *Thiobacillus*. J. Gen. Appl. Microbiol. 30 (3), 211–222.
Kelly, D.P., Postgate, J.R., Kelly, D.P., 1982. Biochemistry of the chemolithotrophic oxidation of inorganic sulphur. Philos. Trans. R. Soc. Lond. B Biol. Sci. 298 (1093), 499–528.
Klatt, J.M., Polerecky, L., 2015. Assessment of the stoichiometry and efficiency of CO_2 fixation coupled to reduced sulfur oxidation. Front. Microbiol. 6, 484.
Kohlhepp, B., Lehmann, R., Seeber, P., Küsel, K., Trumbore, S.E., Totsche, K.U., 2017. Aquifer configuration and geostructural links control the groundwater quality in thin-bedded carbonate–siliciclastic alternations of the Hainich CZE, central Germany. Hydrol. Earth Syst. Sci. 21 (12), 6091–6116.
Kumar, S., Herrmann, M., Blohm, A., Hilke, I., Frosch, T., Trumbore, S.E., Küsel, K., 2018. Thiosulfate- and hydrogen-driven autotrophic denitrification by a microbial consortium enriched from groundwater of an oligotrophic limestone aquifer. FEMS Microbiol. Ecol. 94 (10), fiy141.
Kumar, S., Herrmann, M., Thamdrup, B., Schwab, V.F., Geesink, P., Trumbore, S.E., Totsche, K.U., Küsel, K., 2017. Nitrogen loss from pristine carbonate-rock aquifers of the Hainich Critical Zone Exploratory (Germany) is primarily driven by chemolithoautotrophic Anammox processes. Front. Microbiol. 8, 1951.
Küsel, K., Totsche, K.U., Trumbore, S.E., Lehmann, R., Steinhäuser, C., Herrmann, M., 2016. How deep can surface signals be traced in the critical zone? Merging biodiversity with biogeochemistry research in a Central German Muschelkalk landscape. Front. Earth Sci. 4, 32.
Lehmann, R., Totsche, K.U., 2020. Multi-directional flow dynamics shape groundwater quality in sloping bedrock strata. J. Hydrol. 580, 124291.
Maki, J.S., 2013. Bacterial intracellular sulfur globules: structure and function. Microb. Physiol. 23 (4–5), 270–280.
Marcia, M., Ermler, U., Peng, G., Michel, H., 2010. A new structure-based classification of sulfide: quinone oxidoreductases. Proteins 78 (5), 1073–1083.
Marteinsson, T., Viggó, Rúnarsson, Á., Stefánsson, A., Thorsteinsson, T., Jóhannesson, T., Magnússon, S.H., Reynisson, E., Einarsson, B., Wade, N., Morrison, H.G., Gaidos, E., 2013. Microbial communities in the subglacial waters of the Vatnajökull ice cap, Iceland. ISME J. 7 (2), 427–437.
Matějů, V., Čižinská, S., Krejčí, J., Janoch, T., 1992. Biological water denitrification-a review. Enzym. Microb. Technol. 14 (3), 170–183.
Mikucki, J.A., Lee, P.A., Ghosh, D., Purcell, A.M., Mitchell, A.C., Mankoff, K.D., Fisher, A.T., Tulaczyk, S., Carter, S., Siegfried, M.R., Fricker, H.A., Hodson, T., Coenen, J., Powell, R., Scherer, R., Vick-Majors, T., Achberger, A.A., Christner, B.C., Tranter, M., 2016. Subglacial Lake Whillans microbial biogeochemistry: a synthesis of current knowledge. Philos. Trans. Math. Phys. Eng. Sci. 374 (2059), 20140290.
Mosley, O.E., Gios, E., Close, M., Weaver, L., Daughney, C., Handley, K.M., 2022. Nitrogen cycling and microbial cooperation in the terrestrial subsurface. ISME J. 16 (11), 2561–2573.
Overholt, W.A., Trumbore, S., Xu, X.M., Bornemann, T.L.V., Probst, A.J., Krüger, M., Herrmann, M., Thamdrup, B., Bristow, L.A., Taubert, M., Schwab, V.F., Hölzer, M., Marz, M., Küsel, K., 2022. Carbon fixation rates in groundwater similar to those in oligotrophic marine systems. Nat. Geosci. 15 (7), 561–567.
Pande, S., Kost, C., 2017. Bacterial unculturability and the formation of intercellular metabolic networks. Trends Microbiol. 25 (5), 349–361.
Pitcher, R.S., Watmough, N.J., 2004. The bacterial cytochrome cbb3 oxidases. Biochim. Biophys. Acta Bioenerg. 1655, 388–399.
Pu, J., Feng, C., Liu, Y., Li, R., Kong, Z., Chen, N., Tong, S., Hao, C., Liu, Y., 2014. Pyrite-based autotrophic denitrification for remediation of nitrate contaminated groundwater. Bioresour. Technol. 173, 117–123.
Rimstidt, J.D., Vaughan, D.J., 2003. Pyrite oxidation: a state-of-the-art assessment of the reaction mechanism. Geochim. Cosmochim. Acta 67 (5), 873–880.
Russ, L., Speth, D.R., Jetten, M.S.M., Op den Camp, H.J.M., Kartal, B., 2014. Interactions between anaerobic ammonium and sulfur-oxidizing bacteria in a laboratory scale model system. Environ. Microbiol. 16 (11), 3487–3498.
Schwedt, A., Kreutzmann, A.C., Polerecky, L., Schulz-Vogt, H.N., 2012. Sulfur respiration in a marine chemolithoautotrophic *Beggiatoa* strain. Front. Microbiol. 2, 276.
Shah, V., Zhao, X., Lundeen, R.A., Ingalls, A.E., Nicastro, D., Morris, R.M., 2019. Morphological plasticity in a sulfur-oxidizing marine bacterium from the SUP05 clade enhances dark carbon fixation. mBio 10 (3), e00216–e00219.
Sierra-Alvarez, R., Beristain-Cardoso, R., Salazar, M., Gómez, J., Razo-Flores, E., Field, J.A., 2007. Chemolithotrophic denitrification with elemental sulfur for groundwater treatment. Water Res. 41 (6), 1253–1262.
Song, N., Cai, H.Y., Yan, Z.S., Jiang, H.L., 2013. Cellulose degradation by one mesophilic strain *Caulobacter* sp. FMC1 under both aerobic and anaerobic conditions. Bioresour. Technol. 131, 281–287.
Stewart, V., Lu, Y., Darwin, A.J., 2002. Periplasmic nitrate reductase (NapABC enzyme) supports anaerobic respiration by *Escherichia coli* K-12. J. Bacteriol. 184 (5), 1314–1323.
Taubert, M., Overholt, W.A., Heinze, B.M., Matanfack, G.A., Houhou, R., Jehmlich, N., von Bergen, M., Rösch, P., Popp, J., Küsel, K., 2022. Bolstering fitness via CO_2 fixation and organic carbon uptake: mixotrophs in modern groundwater. ISME J. 16 (4), 1153–1162.
Taubert, M., Stöckel, S., Geesink, P., Girnus, S., Jehmlich, N., von Bergen, M., Rösch, P., Popp, J., Küsel, K., 2018. Tracking active groundwater microbes with D_2O labelling to understand their ecosystem function. Environ. Microbiol. 20 (1), 369–384.
Taubert, M., Vogt, C., Wubet, T., Kleinsteuber, S., Tarkka, M.T., Harms, H., Buscot, F., Richnow, H.H., von Bergen, M., Seifert, J., 2012. Protein-SIP enables time-resolved analysis of the carbon flux in a sulfate-reducing, benzene-degrading microbial consortium. ISME J. 6 (12), 2291–2301.
Wegner, C.E., Gaspar, M., Geesink, P., Herrmann, M., Marz, M., Küsel, K., 2019. Biogeochemical regimes in shallow aquifers reflect the metabolic coupling of the elements nitrogen, sulfur, and carbon. Appl. Environ. Microbiol. 85 (5), e02346. -02318.
Welte, C., Hafner, S., Krätzer, C., Quentmeier, A., Friedrich, C.G., Dahl, C., 2009. Interaction between Sox proteins of two physiologically distinct bacteria and a new protein involved in thiosulfate oxidation. FEBS Lett. 583 (8), 1281–1286.
Yan, L., Hermans, S.M., Totsche, K.U., Lehmann, R., Herrmann, M., Küsel, K., 2021. Groundwater bacterial communities evolve over time in response to recharge. Water Res. 201, 117290.
Yang, T., Lyons, S., Aguilar, C., Cuhel, R., Teske, A., 2011. Microbial communities and chemosynthesis in Yellowstone Lake sublacustrine hydrothermal vent waters. Front. Microbiol. 2, 130.
Zhao, T., Li, Y., Zhang, Y., 2021. Biological carbon fixation: a thermodynamic perspective. Green Chem. 23 (20), 7852–7864.

CORRECTED PROOF